Organic Electronics 14 (2013) 2014–2022

Contents lists available at SciVerse ScienceDirect

Organic Electronics

journal homepage: www.elsevier.com/locate/orgel

Color stable multilayer all-phosphor white organic light-emitting diodes with excellent color quality

Shiming Zhang [a,b,*], Shouzhen Yue [a], Qingyang Wu [a], Zhensong Zhang [a], Yu Chen [a], Xuehui Wang [a], Ziyang Liu [a], Guohua Xie [c], Qin Xue [d], Dalong Qu [a], Yi Zhao [a,*], Shiyong Liu [a]

[a] State Key laboratory on Integrated Optoelectronics, College of Electronic Science and Engineering, Jilin University, Changchun 130012, People's Republic of China
[b] Département of Chemical Engineering, École Polytechnique de Montréal, Montréal, Québec, Canada H3C 3J7
[c] Institut für Angewandte Photophysik, Technische Universtität Dresden, 01062 Dresden, Germany
[d] College of Physical Science and Technology, Central China Normal University, Wuhan 430079, People's Republic of China

ARTICLE INFO

Article history:
Received 28 October 2012
Received in revised form 30 March 2013
Accepted 18 April 2013
Available online 3 May 2013

Keywords:
WOLED
All-phosphor
Multilayer
Stable
$Ir(ppz)_3$
CRI

ABSTRACT

The color stability of all-phosphor white organic light-emitting diodes (WOLEDs) is crucial and remains a challenge that must be overcome before the wide application of phosphor WOLEDs technology. Besides, color stable all-phosphor WOLEDs should also offer high color rendering index (CRI) and ideal correlated color temperature (CCT) simultaneously to make the technology competitive against other alternative technologies such as inorganic LEDs. In this work, we demonstrate a series of color stable all-phosphor WOLEDs with two emitters (blue and yellow), three emitters (blue, green/red, and yellow) and four emitters (blue, green, yellow and red) by introducing tris (phenylpyrazole) Iridium [$Ir(ppz)_3$] as interlayer. The results show that appropriate thickness of $Ir(ppz)_3$ interlayer not only can control exciton distribution in the emission zone, but also can improve the spectra stability. In particular, one efficient four-color device with double-interlayer yields fairly high CRI of 92 and 90, ideal CCT of 3703 K and 3962 K at illumination-relevant luminance of 100 cd m^{-2} and 1000 cd m^{-2}, respectively, which is very appropriate to indoor lighting application. By further employing appropriate hosts to regulate the carrier injection, ultrahigh stable four-color devices with applicable CRI are finally achieved.

1. Introduction

White organic light-emitting diodes (WOLEDs) have drawn particular attention due to their potential applications in solid-state lighting and flat panel display [1,2]. Up to now, lots of works have been carried out to improve the performances of WOLEDs: fluorescent-tube efficiency has been achieved in WOLEDs by Karl Leo's group and WOLEDs with a projected lifetime of 100,000 h have been demonstrated by Universal Display Corporation [3,4]. However, in addition to the complications encountered in the field of flat-panel displays: such as device stability, cost of manufacturing and patternability, lighting applications pose further challenges: the WOLEDs must provide high efficiency, ideal correlated color temperature (CCT), high color rendering index (CRI) as well as high color stability [5–7]. The color-point has to remain stable both over the entire operational lifetime of the device and for different brightness levels [7]. Even applications for television display, the device is also required to have a negligible color shift at video brightness [8]. However, the stability issue of the organic devices by far remains a major challenge. Generally, the color stability of WOLEDs is difficult to maintain due to imbalanced color emission under different applied voltages, and it is much more difficult to get the

* Corresponding authors Address: State Key laboratory on Integrated Optoelectronics, College of Electronic Science and Engineering, Jilin University, Changchun 130012, People's Republic of China (Y. Zhao). Tel.: +1 438 8629185, +86 431 85168242 8301.
E-mail addresses: shiming.zhang@polymtl.ca (S. Zhang), yizhao@jlu.edu.cn (Y. Zhao).

1566-1199/$ - see front matter © 2013 Elsevier B.V. All rights reserved.
http://dx.doi.org/10.1016/j.orgel.2013.04.039

color stability in three or more color WOLEDs [9,10]. To date, various approaches towards realizing high stability WOLEDs have been reported and several groups claimed to have demonstrated devices that provide color-stable white emission over large brightness level ranges [6,11–16]. Among these approaches, adopting all-phosphor, multiple emission layers (M-EML) architecture has great potential because electrophosphorescence can, in theory, achieve unity internal quantum efficiency through harvesting both singlet and triplet excitons, and M-EML structure has advantages over other architectures in terms of efficiency and color controllability [6,17]. In addition, WOLEDs with separate EMLs for primary colors red (R), yellow (Y), green (G), and blue (B) are more useful for full-color displays [18]. However, one of the major challenges facing all-phosphor M-EML WOLEDs is to reduce the color shift with increasing luminance and achieve high CRI and ideal CCT simultaneously in order to satisfy practical application. Therefore, further study on phosphor M-EML WOLEDs to develop high color stability with excellent color quality is considerably significant.

In this work, we report the achievement of a series of color-stable all-phosphor M-EML WOLEDs by introducing tris (phenylpyrazole) Iridium [Ir(ppz)$_3$] as interlayer in the EMLs. A detailed study was carried out to analysis the effect of Ir(ppz)$_3$ interlayer thickness on the device performance. Through rational design, efficient four-color device with high and durable CRI about 90 over 100 cd m^{-2} to 1000 cd m^{-2}, and ideal warm CCT around 4000 K, which is very appropriate to indoor lighting application, is obtained [6,19]. Further, ultra-stable four-color all-phosphor WOLEDs with acceptable CRI value is finally realized by utilizing appropriate host materials to adjust carrier injection. The Commission Internationale de L'Eclairage (CIE) coordinates of the best device only change marginally from (0.388, 0.455) to (0.384, 0.451) over 100 cd m^{-2} to 10,000 cd m^{-2}, and the variation is only (±0.000, ±0.001) over the illumination-relevant luminance of 100 cd m^{-2} and 1000 cd m^{-2}, which is one of the best results among the M-EML all-phosphor WOLEDs reported in literatures so far.

2. Experimental section

The materials used for device fabrication were obtained through commercial sources and used without further purification. Prior to the device fabrication, the patterned ITO-coated glass (20 Ω square^{-1}) substrates were scrubbed and sonicated consecutively with acetone, ethanol, and deionized water, respectively. All the organic layers were thermally deposited in vacuum (~4.0 × 10^{-4} Pa) at a rate of 1–2 Å s^{-1} monitored in situ with the quartz oscillator. 4,4,4-tris(3-methylphenylphenylamino)-triphenylamine (m-MTDATA) and 7-dipheny-1,10-phenanthroline (BPhen) were used as hole injection layer (HIL), and hole-blocking layer (HBL)/electron-transporting layer (ETL), respectively. Tris(phe-nylpyrazole)irid-ium [Ir (ppz)$_3$] was served as hole-transporting layer and interlayer. Iridium(III)

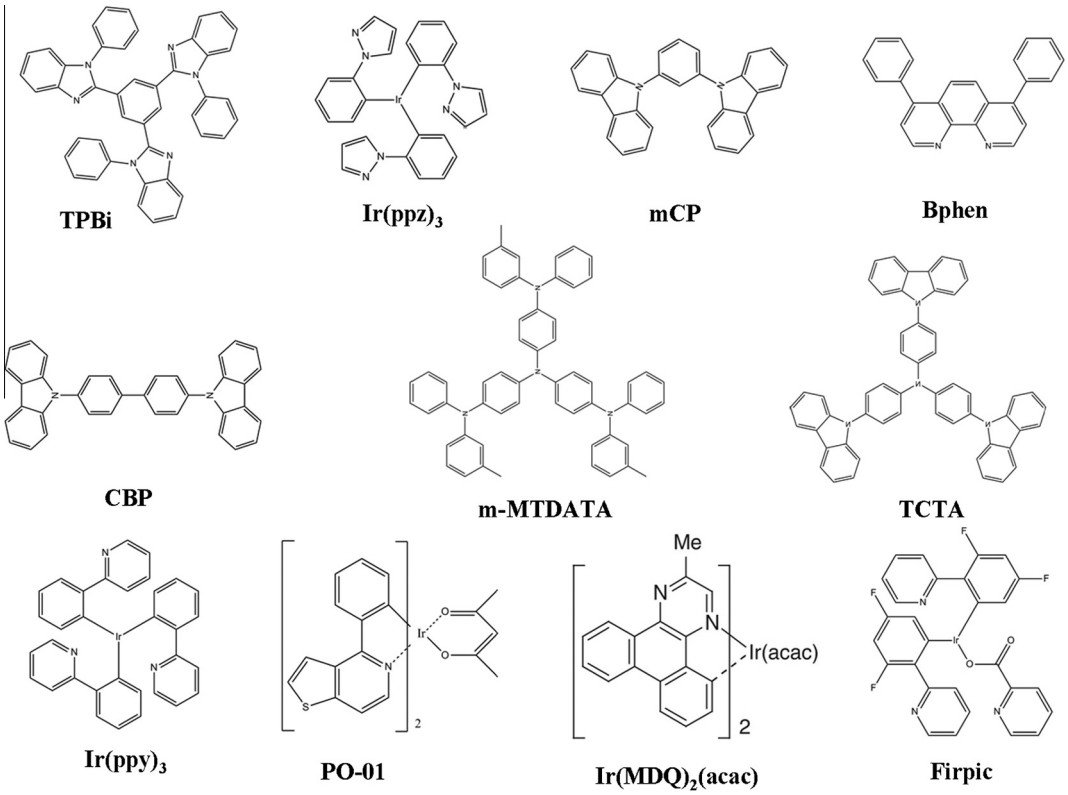

Scheme 1. The chemical structures of the compounds used.

Table 1
Detailed device structures studied in this work.

Device	HTL (nm)	EML (nm, wt.%)		(nm)	ETL (nm)
W1	ITO/m-MTDATA (45)/ Ir $(ppz)_3$ (10)	CBP: PO-01 (5, 6%)/Ir $(ppz)_3$ (x)/mCP: Firpic (5, 8%)	$W_{1\text{-}1}$	$x = 0$	Bphen (40)/ LiF(1)/Al (100)
			$W_{1\text{-}2}$	$x = 0.5$	
			$W_{1\text{-}3}$	$x = 1$	
			$W_{1\text{-}4}$	$x = 2$	
W2	ITO/m-MTDATA (45)/ Ir $(ppz)_3$ (10)	CBP: Ir$(ppy)_3$ (3, 8%)/Ir $(ppz)_3$ (y)/mCP: Firpic (5, 8%)/CBP: PO-01 (5, 6%)	$W_{2\text{-}1}$	$y = 1$	
			$W_{2\text{-}2}$	$y = 2$	
			$W_{2\text{-}3}$	$y = 3$	
			$W_{2\text{-}4}$	$y = 4$	
		CBP: Ir$(MDQ)_2$(acac) (3, 6%)/Ir $(ppz)_3$ (z)/mCP: Firpic (5, 8%)/CBP: PO-01 (5, 6%)	$W_{2\text{-}5}$	$z = 2$	
W3	ITO/m-MTDATA (45)/ Ir $(ppz)_3$ (10)	CBP: Ir$(ppy)_3$ (5, 8%)/Ir $(ppz)_3$ (2)/CBP: Ir$(MDQ)_2$(acac) (5, 6%)/Ir $(ppz)_3$ (2)/ mCP: Firpic (5, 8%)/CBP: PO-01 (5, 6%)			
W4	ITO/m-MTDATA (45)/ Ir $(ppz)_3$ (10)	CBP: Ir$(MDQ)_2$(acac) (5, 6%)/Ir $(ppz)_3$ (2)/CBP: Ir$(ppy)_3$ (5, 8%)/ Ir $(ppz)_3$ (2)/ mCP: Firpic (5, 8%)/CBP: PO-01 (5, 6%)			
W5	ITO/m-MTDATA (45)/ Ir $(ppz)_3$ (10)	TCTA: Ir$(MDQ)_2$(acac) (5, 6%)/Ir $(ppz)_3$ (γ)/TPBi: Ir$(ppy)_3$ (5, 8%)/ Ir $(ppz)_3$ (2)/mCP: Firpic (5, 15%)/CBP: PO-01 (5, 6%)	$W_{5\text{-}1}$	$\gamma = 0$	
			$W_{5\text{-}2}$	$\gamma = 0.5$	
			$W_{5\text{-}3}$	$\gamma = 1$	
			$W_{5\text{-}4}$	$\gamma = 2$	

bis(2-methyldibenzo-[f, h]quinoxaline) (acetylacetonate) [Ir $(MDQ)_2$(acac)], Tris(2-phenylpyridine)iridium [Ir $(ppy)_3$], Iridium(III) bis(4-phenylthieno[3, 2-c] pyridinato-N,$C^{2'}$) acetylacetonate (PO-01) and Iridium(III) bis[(4,6-difluo-rophenyl)-pyridinato-N,C^{2-}] (Firpic) were used as R, G, Y, and B triplet emitters, respectively. 4,4-N,N-dicarbazole-biphenyl (CBP) and N,N′-dicarbazolyl-3,5-benzene (mCP) were served as hosts materials. The highest occupied molecular orbital (HOMO) and the lowest unoccupied molecular orbital (LUMO) levels of organic materials are obtained from literatures [3,20–22]. The chemical structures used in this paper are shown in Scheme 1. The detailed device structures and energy levels of the materials used are shown in Table 1 and Fig. 1. After the deposition of LiF, the samples were transferred to metal chamber, and suffered from a vacuum break and exposed to the ambient atmosphere for ~10 min due to the change of the shadow masks to determine the active area. The current–voltage-forward luminance characteristics and CIE coordinates were measured with a PR650 Spectrascan spectrometer and a Keithley 2400 programmable voltage-current source. CRI and CCT values were calculated with software SETFOS 3.0 from FLUXIM AG. All the samples were measured directly after fabrication without encapsulation in ambient atmosphere at room temperature.

3. Results and discussions

We first demonstrated complementary-color phosphor devices with Firpic and PO-01 combinations by utilizing Ir $(ppz)_3$ as interlayer (W1). The corresponding normalized electroluminescent (EL) spectra at different applied voltages are shown in Fig. 2. We can clearly see that introduction of Ir$(ppz)_3$ interlayer could efficiently block electrons for the B-EML and accordingly balanced the white emission due to its intrinsic higher LUMO energy level and triplet level [20]. In addition, relative stable EL spectra can be maintained.

In succession, three-color white devices (W2) were fabricated and further studied. The Y-EML was placed closer to the cathode side relative to the B-EML in order to form an exciton recombination zone for PO-01 due to the inherent energy level offsets existed between mCP and CBP. The Ir$(ppz)_3$ interlayer thickness was varied from 1 nm to 4 nm here to reveal its effect on the spectra stability. Fig. 3a demonstrates the non-normalized EL spectra of W2 at a current density of 25 mA cm^{-2}. As depicted, the emission intensity of Ir$(ppy)_3$ decreases with that of Firpic increases when the Ir$(ppz)_3$ thickness increases from 1 nm to 3 nm, while when we further increase the Ir$(ppz)_3$ thickness up to 4 nm, the Firpic emission intensity remains nearly unchanged. This phenomenon indicates that 3 nm Ir$(ppz)_3$ is sufficient to retain electrons for Firpic emission. However, as the spectra shown in Fig. 3b, despite 3 nm Ir$(ppz)_3$ can realize sufficient B-emission, it seriously worsens the spectra stability of the devices (W2-3/W2-4). In contrast, devices with 1 nm or 2 nm Ir$(ppz)_3$ interlayer (W2-1/W2-2) show rather high EL spectra stability. These results point to the key conclusion of this work, to obtain stable EL spectra, Ir$(ppz)_3$ thickness should be less than 2 nm.

In the following, we fixed the Ir$(ppz)_3$ interlayer thickness at 2 nm, and replaced the G-EML by R-EML (W2-5) aiming to examine the above conclusion. As shown in Fig. 3c, W2-5 not only exhibits stable spectra as expected, but also displays CRI higher than 70 between 100 and 1000 cd m^{-2} (Table 2).

To further improve the CRI, four-color devices with double Ir$(ppz)_3$ interlayer (W3 and W4) were presented. Compared with device W3, the G-EML exchanged positions with the R-EML in device W4. As shown in Fig. 4a and Table 2, W3 exhibits excellent white color with four separated emissive peaks, which are originated from R–Y–G–B EML, respectively. The CIE coordinates change from (0.402, 0.409) to (0.383, 0.420) as the luminance varied from 100 cd m^{-2} to 10,000 cd m^{-2}. More significantly, the CRI value of W3 reaches as high as 92 at 100 cd m^{-2} with a current efficiency (CE) of 20.9 cd A^{-1} and an ideal warm CCT of

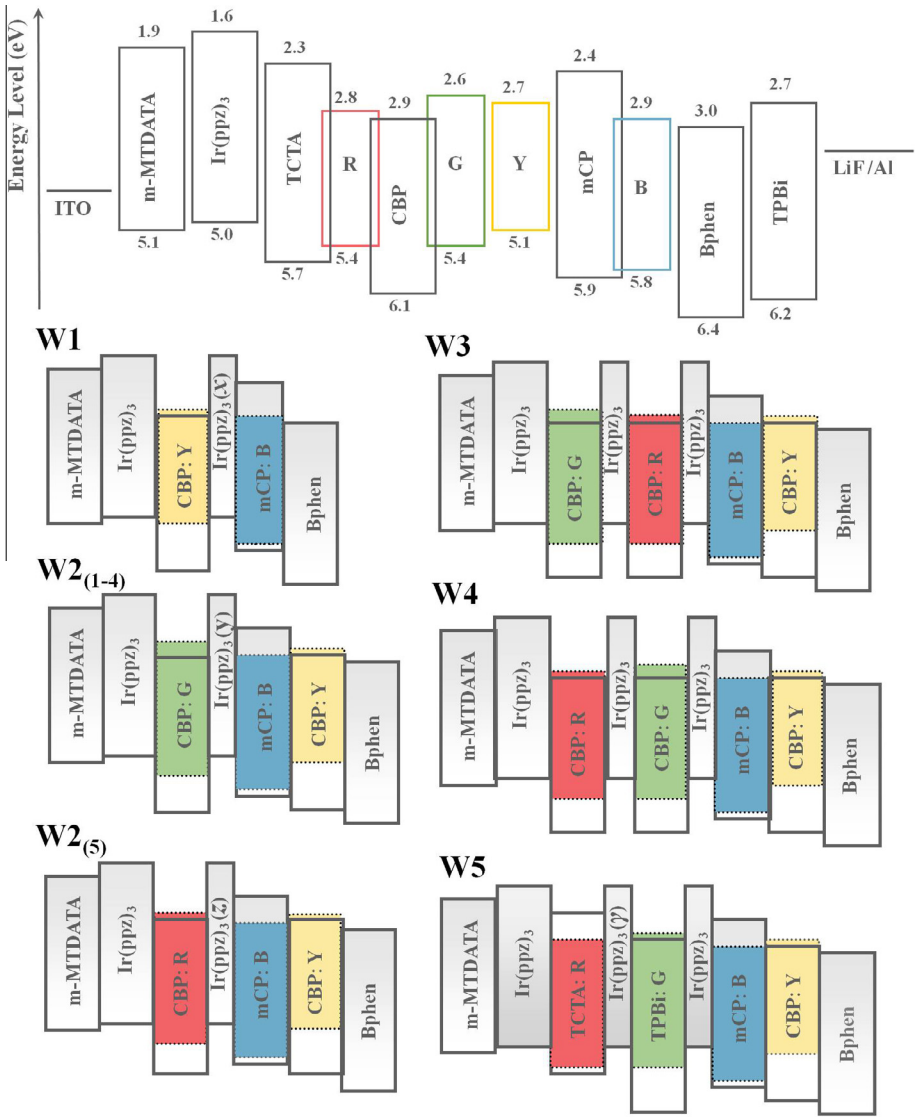

Fig. 1. Energy level diagrams and device configurations for WOLEDs studied in this paper.

3703 K. For the technically most relevant luminance range between 100 cd m^{-2} and 1000 cd m^{-2}, the CRI can be maintained over 90, which is very appropriate to indoor lighting application [19]. According to the data summarized by Jwo-Huei Jou and co-workers, the overall (electrical and optical) performance of W3, considering both efficiency and CRI, is one of the best WOLEDs reported so far [23]. In contrast, however, although W4 can also produce stable color emission, its spectra is quite different from W3. It can be clearly seen that W4 shows predominantly PO-01 emission, the Firpic emission is greatly suppressed as compared to W3 and we can hardly observe the emission from $Ir(MDQ)_2(acac)$. Therefore, W4 shows lower CRI about 60 with CCT around 4400 K despite the CE being as high as 34.4 cd A^{-1} at 1000 cd m^{-2} due to the strong emission of the efficient emitter of PO-01 [24].

In order to elucidate the origin of the spectra difference between W3 and W4, electron-only and hole-only devices were prepared. We can see from Fig. 5a that an obvious reduction of the electron mobility can be observed upon doping of $Ir(MDQ)_2(acac)$ into CBP, which indicates that $Ir(MDQ)_2(acac)$ into CBP served as a trapping site for electrons, whereas doping $Ir(ppy)_3$ into CBP has almost no influence on electron transport. The above phenomena provide us a hint to explain the above difference. As we know, CBP is a bipolar charge transport host and possesses relatively higher electron mobility [25]. For device W4, the electrons accumulated at the B-EML/$Ir(ppz)_3$ interface can easily be transported to the G-EML/$Ir(ppz)_3$ interface to emit G-color once they hop over the barrier between CBP and $Ir(ppz)_3$ due to the good electron-transporting property of CBP. However, fewer electrons can be further transferred and utilized by $Ir(MDQ)_2(acac)$ molecules to harvest R-color due to the effective exciton gathering ability of $Ir(ppy)_3$. While for W3, electrons travel through the B-EML will immediately be trapped by

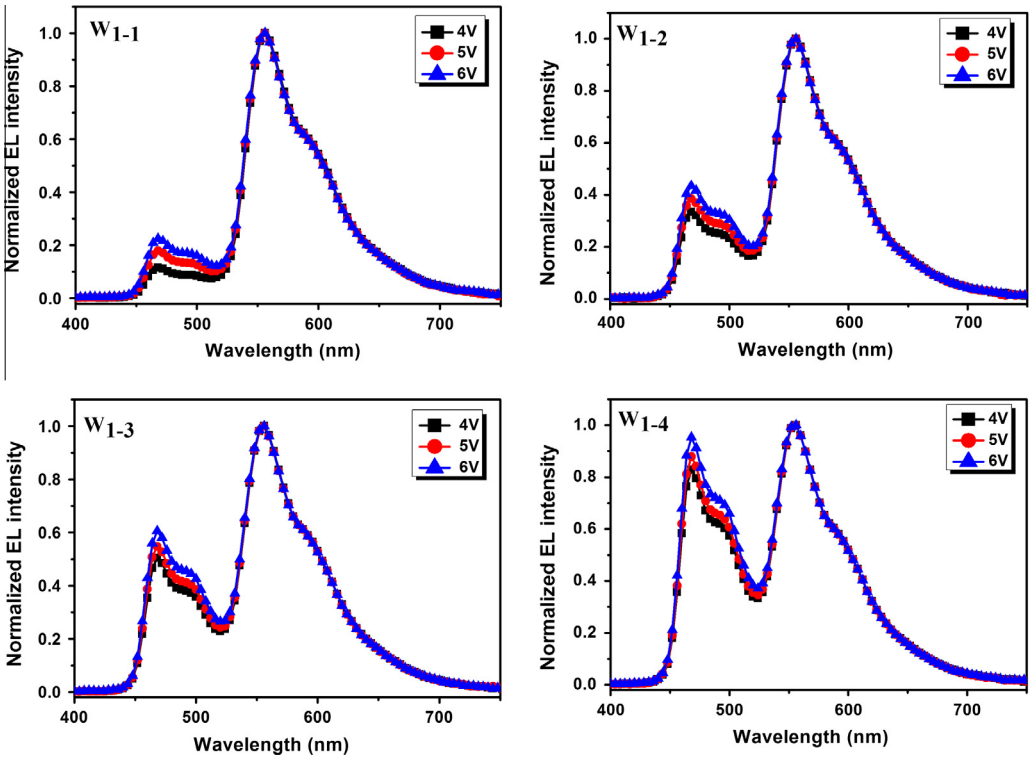

Fig. 2. Comparison of the EL spectra characteristics of device W1 at different applied voltages (corresponding to 10^2 cd m^{-2} to 10^4 cd m^{-2}).

$Ir(MDQ)_2(acac)$ molecules to emit R-color, which will strongly obstruct the transport of electrons and should also account for the lower current density as compared with W4 (Fig. 4b). The trapped electrons will subsequently create a strong reverse built-in electric field to further restrain electron injection/transport from B-EML to R-EML. Hence, a much higher electron density can be retained in the B-EML, leading to a strong Firpic emission in W3 inevitably.

Balanced carrier injection accomplished by assistance electron-transporting on emitter molecule may be one of the hidden reasons for the stability of the above devices. As is known, electron is normally minor carrier compared with hole within an OLED, and its efficient transport plays a pivotal role in obtaining a stable device. Depicted in Fig. 5a, doping PO-01 into CBP shows much higher electron mobility compared with pure CBP, and Firpic in mCP offers a good channel for electron transporting [26]. These results suggest that there is another efficient continuous electron-transporting channel formed on the emitter molecules, which can greatly facilitate electron injection/transport to the EML and avoid spectral instability caused by electron-trapping. Moreover, from the point of view of the holes, the trapping behavior of $Ir(MDQ)_2(acac)$ and $Ir(ppy)_3$ both reduce the hole transport mobility in CBP (Fig. 5b), which will impede the hole injection. In addition, this hole-trapping of the emitters can also reduce the accumulation of holes in the EML, lowering the formation of h^+ polarons and thereby avoiding severe efficiency roll-off problem at high luminance [27]. The minor decrease in the intensity of the R-color with increasing luminance in W3 is due to the reduced carrier trapping ability as applied voltage increased [28], which is the primary light emission mechanism of $Ir(MDQ)_2(acac)$.

Based on the above analysis, to ameliorate the color quality of W4, we subsequently employed 1,3,5-tris(2-N-phenylbenzimidazolyl)benzene (TPBi) to replace CBP as the host for $Ir(ppy)_3$ (W5) to promote electron further injection into the R-EML to realize R-emission. In this case, however, both hole and electron density will be high at the $Ir(ppz)_3$/R-EML interface, which may cause a strong exciton annihilation there. To solve this conflict, hole transport material 4,4,4-tris(N-carbazolyl)-triphenylamine (TCTA), which is an efficient host for $Ir(MDQ)_2(acac)$, was utilized to promote hole transport to the G-EML. It should be mentioned that although TPBi is a typical electron transport material, holes can be transported from the G-EML to the following EML because the obvious hole-transporting assistance behavior of $Ir(ppy)_3$ in TPBi (Fig. 6a).

As can be seen in Fig. 6b, in a rather wide range of luminance, W5 realizes ultra-stable four-color white emission. The $Ir(ppz)_3$ thickness variation between the G-EML and R-EML can smartly adjust the relative emission intensity of these two colors, but almost has no influence on the spectra stability. Typically, the CIE coordinates of W5-1 only change marginally from (0.388, 0.455) to (0.384, 0.451) over 100 cd m^{-2} to 10,000 cd m^{-2}, and the variation is only (±0.000, ±0.001) over the illumination-relevant luminance of 100 cd m^{-2} and 1000 cd m^{-2}. CRI of W5–1 is increased up to more than 80 with warm CCT values about 4200 K (Table 2), which satisfy the requirements for practical

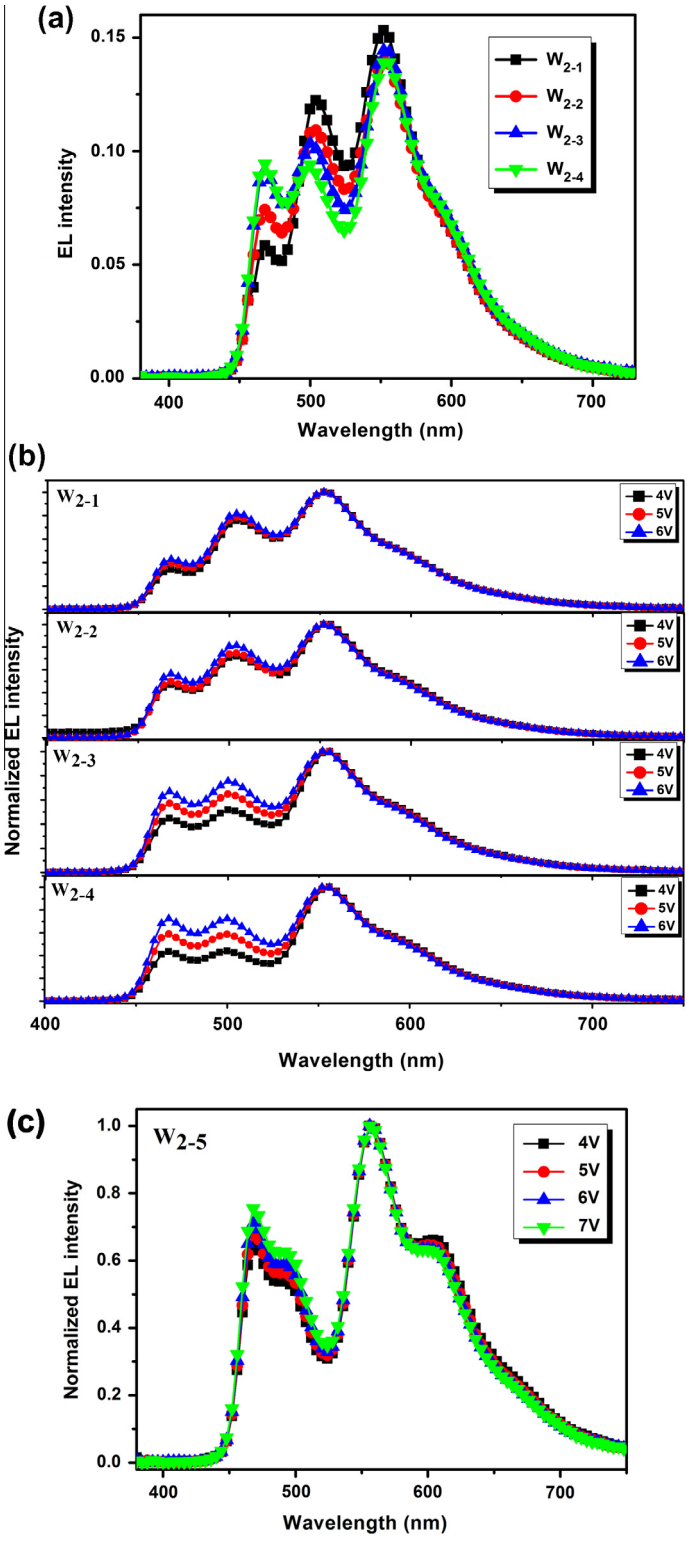

Fig. 3. Summary of the characteristics of the device W2: (a) Non-normalized EL spectra of W2-1–W2-4 at a current density of 25 mA cm^{-2}, (b) normalized EL spectra of W2-1–W2-4 and (c) normalized EL spectra of W2-5.

indoor lighting. In particular, the CE of W5-1 reaches 28.5 cd A^{-1} at 100 cd m^{-2} and the value can be maintained at 28.1 cd A^{-1} at 1000 cd m^{-2} (Fig. 6c). The efficiency increase from W5-1 to W5-4 is due to the stronger $Ir(ppy)_3$

Table 2
Summary of WOLEDs performances studied in this work.

Device	Current efficiency[a] (cd A^{-1})	Power efficiency[a] (lm W^{-1})	EQE[a] (%)	CIE (x, y)[a]	CRI[b]	CCT[b] (K)
W1-3	22.3/24.6/17.1	20.0/17.1/9.0	8..2/8.5/7.3	(0.380, 0.458), (0.376, 0.455), (0.366, 0.447)	54, 55	4544, 4601
W2-3	33.4/32.8/25.5	26.5/22.9/13.3	11.1/10.9/8.9	(0.363, 0.478), (0.353, 0.473), (0.329, 0.462)	55, 56	4826, 5242
W2-5	14.6/18.2/14.0	10.2/10.4/5.2	7.1/8.2/6.1	(0.386, 0.433), (0.380, 0.431), (0.362, 0.423)	71, 70	4164, 4290
W3	20.9/20.1/14.9	12.0/8.5/4.6	10.5/10.3/6.2	(0.402, 0.409), (0.394, 0.413), (0.383, 0.420)	92, 90	3703, 3962
W4	26.6/34.4/25.2	20.9/21.6/11.3	10.4/11.4/9.1	(0.388, 0.472), (0.383, 0.470), (0.374, 0.463)	58, 60	4326, 4414
W5-1	28.5/28.1/23.7	20.0/17.7/10.6	11.6/11.5/9.5	(0.388, 0.455), (0.387, 0.453), (0.384, 0.451)	81, 80	4241, 4287

[a] Current efficiency, power efficiency, external quantum efficiency (EQE) and CIE (x, y) coordinates at 100 cd m^{-2}, 1000 cd m^{-2} and 10,000 cd m^{-2}, respectively;
[b] CRI and CCT values at 100 cd m^{-2} and 1000 cd m^{-2}.

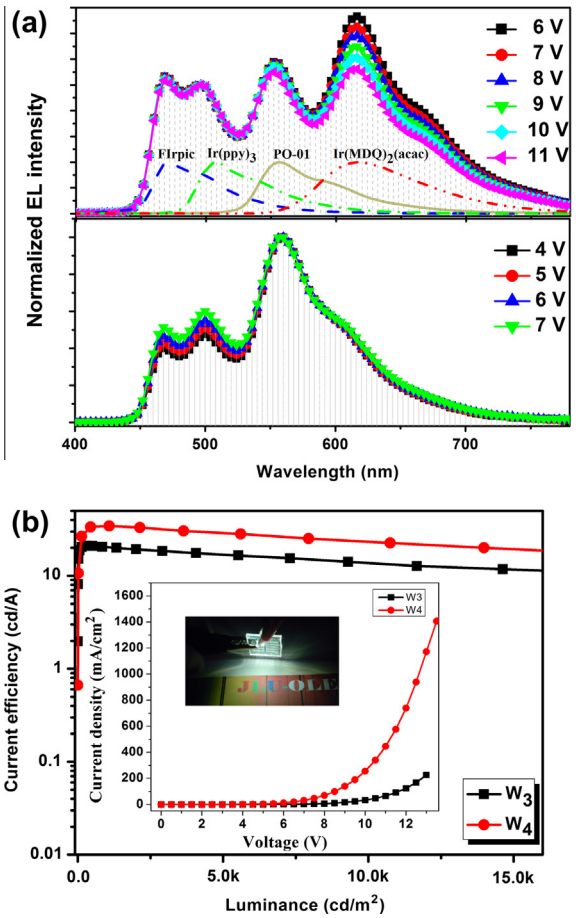

Fig. 4. (a) EL spectra of W3 (upper) and W4 (lower); Dash-dot lines refer to the EL spectra of OLEDs with a single emitting layer and (b) CE versus luminance curves of W3 and W4. The insets show J–V curves of W3 and W4 and an image of W3 with active area of 4.0 mm^2.

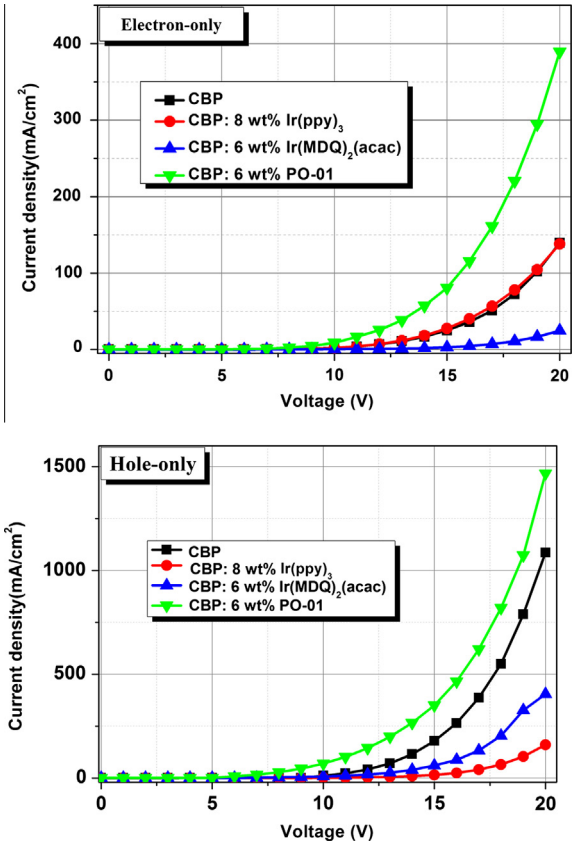

Fig. 5. Current density versus voltage characteristics of (a) electron-only devices: ITO/LiF(1 nm)/Bphen (40 nm)/Ir(ppz)$_3$ (2 nm)/X (40 nm)/Bphen (40 nm)/LiF (1 nm)/Al and (b) hole-only devices: ITO/MoO_3 (10 nm)/NPB (40 nm)/Ir(ppz)$_3$ (2 nm)/X (40 nm)/NPB (40 nm)/MoO_3 (10 nm)/Al. Here X are CBP, CBP: 8 wt.% Ir(ppy)$_3$, CBP: 6 wt.% Ir(MDQ)$_2$(acac), and CBP: 6 wt.% PO-01, respectively.

emission, which, however, unbalances the spectra and accounts for the consecutive CRI drops (<80).

It is worth-mentioning that the device efficiency studied in this work is only measured in the forward direction without the use of an integrating sphere or outcoupling. When the WOLEDs are used for solid-state lighting, all photons should be taken into account for illumination. In this case, to get the total efficiency, a factor of 1.7–2.3 should be applied to the forward-viewing efficiencies [2,12,29,30]. Therefore, actually, the highest CE of devices W2-3, W3 and W5-1 can reach 76.8, 48.1 and 65.6 cd A^{-1} at 100 cd m^{-2}, respectively. The efficiency of the present device can still be drastically improved by adopting p–i–n structure to achieve more balanced carrier injection and using a periodic outcoupling structure to increase the light

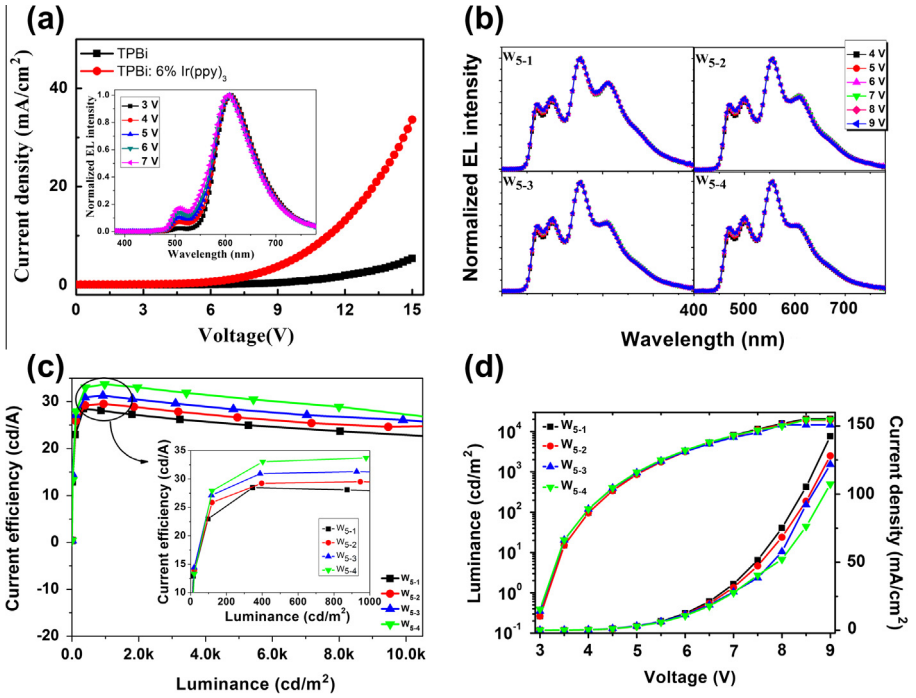

Fig. 6. (a) Hole-only devices: ITO/MoO_3 (10 nm)/NPB (40 nm)/Ir(ppz)$_3$ (2 nm)/X (30 nm)/NPB (40 nm)/MoO_3 (10 nm)/Al. Here X are TPBi, TPBi: 6 wt.% Ir(ppy)$_3$, respectively; The inset shows a control device without Ir(ppz)$_3$ interlayer [ITO/m-MTDATA (45 nm)/Ir (ppz)$_3$ (10 nm)/TCTA: Ir(MDQ)$_2$(acac) (5 nm, 6 wt.%) /TPBi: Ir(ppy)$_3$ (5 nm, 8 wt.%)/mCP: FIrpic (5 nm, 15 wt.%)/CBP: PO-01 (8 nm, 6 wt.%)/Bphen (40 nm)/LiF(1 nm)/Al], (b) normalized EL spectra of W5, (c) CE versus luminance curves of W5 and (d) *V–J–L* curves of W5.

extraction [3,31,32]. We anticipate seeing a more efficient WOLED based on this study in the future.

4. Conclusion

In summary, we have demonstrated a series of color stable M-EML WOLEDs based on all-phosphor emitters using Ir(ppz)$_3$ as interlayer. The results prove that less than 2 nm thickness of Ir(ppz)$_3$ interlayer not only can control exciton distribution in the EML, but also can improve the spectra stability. In particular, an efficient four-color device shows an excellent CRI above 90 with idea CCT values over the illumination-relevant luminance of 100 cd m^{-2} and 1000 cd m^{-2}, making it well suited for lighting applications. High color quality device with excellent color and efficiency stability is eventually implemented by further manipulating carrier transport with appropriate host material to balance carrier injection. We hope this study could further spur the development of stable all-phosphor WOLEDs.

Acknowledgments

We would like to thank all the researchers who participated in this work and whose names appear in references. This work was supported by the National Basic Research Program of China (973 Program) under Grant No. 2010CB327701 and the National Natural Science Foundation of China (Grant Nos. 60977024 and 61275033).

References

[1] B. D'Andrade, M. Thompson, S. Forrest, Adv. Mater. 14 (2002) 147–151.
[2] B. D'Andrade, S. Forrest, Adv. Mater. 16 (2004) 1585–1595.
[3] S. Reineke, F. Lindner, G. Schwartz, N. Seidler, K. Walzer, B. Lussem, K. Leo, Nature 459 (2009) 234–238.
[4] So Franky, Kido Junji, Burrows Paul, Organic Light-Emitting Devices for Solid-State Lighting, Materials Research Society, Warrendale, PA, ETATS-UNIS, 2008.
[5] A.R. Duggal, J.J. Shiang, C.M. Heller, D.F. Foust, Appl. Phys. Lett. 80 (2002) 3470–3472.
[6] Y.-S. Park, J.-W. Kang, D.M. Kang, J.-W. Park, Y.-H. Kim, S.-K. Kwon, J.-J. Kim, Adv. Mater. 20 (2008) 1957–1961.
[7] M.C. Gather, R. Alle, H. Becker, K. Meerholz, Adv. Mater. 19 (2007) 4460–4465.
[8] L. Duan, D. Zhang, K. Wu, X. Huang, L. Wang, Y. Qiu, Adv. Funct. Mater. 21 (2011) 3540–3545.
[9] Y. Shao, Y. Yang, Appl. Phys. Lett. 86 (2005) 073510–073513.
[10] K.S. Yook, S.O. Jeon, C.W. Joo, J.Y. Lee, Appl. Phys. Lett. 93 (2008) 073302–073303.
[11] Y. Sun, N.C. Giebink, H. Kanno, B. Ma, M.E. Thompson, S.R. Forrest, Nature 440 (2006) 908–912.
[12] X. Gong, S. Wang, D. Moses, G.C. Bazan, A.J. Heeger, Adv. Mater. 17 (2005) 2053–2058.
[13] C.-L. Ho, M.-F. Lin, W.-Y. Wong, W.-K. Wong, C.H. Chen, Appl. Phys. Lett. 92 (2008) 083301–083303.
[14] J.-H. Jou, C.-J. Wang, Y.-P. Lin, Y.-C. Chung, P.-H. Chiang, M.-H. Wu, C.-P. Wang, C.-L. Lai, C. Chang, Appl. Phys. Lett. 92 (2008) 223503–223504.
[15] Z. Zhang, G. Xie, S. Yue, Q. Wu, Y. Chen, S. Zhang, L. Zhao, Y. Luo, Y. Zhao, S. Liu, Org. Electron. 13 (2012) 2296–2300.
[16] C.-H. Hsiao, Y.-H. Lan, P.-Y. Lee, T.-L. Chiu, J.-H. Lee, Org. Electron. 12 (2011) 547–555.
[17] S. Gong, Y. Chen, C. Yang, C. Zhong, J. Qin, D. Ma, Adv. Mater. 22 (2010) 5370–5373.
[18] Y.G. Lee, I.S. Kee, H.S. Shim, I.H. Ko, S. Lee, K.H. Koh, Appl. Phys. Lett. 90 (2007) 243503–243508.
[19] M.C. Gather, A. Köhnen, K. Meerholz, Adv. Mater. 23 (2011) 233–248.

[20] G. Xie, Z. Zhang, Q. Xue, S. Zhang, Y. Luo, L. Zhao, Q. Wu, P. Chen, B. Quan, Y. Zhao, S. Liu, J. Phys. Chem. C 115 (2010) 264–269.
[21] P. Chen, Appl. Phys. Lett. 91 (2007) 023505.
[22] S. Kumar, S.-M. Shen, S.-H. Chen, C.-C. Wang, C.-C. Chen, J.-H. Jou, 2012 IACSIT Coimbatore Conferences, 2012, pp. 117–121.
[23] J.-H. Jou, S.-M. Shen, C.-R. Lin, Y.-S. Wang, Y.-C. Chou, S.-Z. Chen, Y.-C. Jou, Org. Electron. 12 (2011) 865–868.
[24] K.-H.S. Heh-Lung Huang, Miao-Cai Jhu, Mei-Rurng Tseng, Jia-Ming Liu, MRS Proceedings, 846, DD9.5, doi:10.1557/PROC-846-DD9.5, 2004.
[25] T. Yamada, F. Suzuki, A. Goto, T. Sato, K. Tanaka, H. Kaji, Org. Electron. 12 (2011) 169–178.
[26] J. Zhao, J. Yu, X. Hu, M. Hou, Y. Jiang, Thin Solid Films 520 (2012) 4003–4007.
[27] Y. Chen, J. Chen, Y. Zhao, D. Ma, Appl. Phys. Lett. 100 (2012) 213301–213304.
[28] Q. Wang, J. Ding, D. Ma, Y. Cheng, L. Wang, X. Jing, F. Wang, Adv. Funct. Mater. 19 (2009) 84–95.
[29] B.W. D'Andrade, R.J. Holmes, S.R. Forrest, Adv. Mater. 16 (2004) 624–628.
[30] H. Wu, G. Zhou, J. Zou, C.-L. Ho, W.-Y. Wong, W. Yang, J. Peng, Y. Cao, Adv. Mater. 21 (2009) 4181–4184.
[31] G. He, M. Pfeiffer, K. Leo, M. Hofmann, J. Birnstock, R. Pudzich, J. Salbeck, Appl. Phys. Lett. 85 (2004) 3911.
[32] Y. Jin, J. Feng, X.-L. Zhang, Y.-G. Bi, Y. Bai, L. Chen, T. Lan, Y.-F. Liu, Q.-D. Chen, H.-B. Sun, Adv. Mater. 24 (2012) 1187–1191.